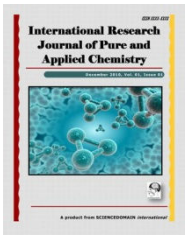

International Research Journal of Pure & Applied Chemistry
1(3): 84-103, 2011

SCIENCEDOMAIN *international*
www.sciencedomain.org

Studies on Characterization and Photocatalytic Activities of Visible Light Sensitive TiO_2 Nano Catalysts Co-doped with Magnesium and Copper

Teshome Abdo Segne[1*], Siva Rao Tirukkovalluri[1] and Subrahmanyam Challapalli[2]

[1]Department of Inorganic & Analytical Chemistry, School of Chemistry, Andhra University, Visakhapatnam, India.
[2]Department of Chemistry, Indian Institute of Technology, Hyderabad, India.

Research Article

Received 22nd June 2011
Accepted 4th August 2011
Online Ready 13th August 2011

ABSTRACT

TiO_2 (anatase) – based photocatalyst powders containing up to 1.00 wt% of magnesium(II) and copper(II) were synthesized using sol– gel method. The powders were characterized by UV–visible Diffuse Reflectance Spectroscopy (DRS), X-ray diffraction (XRD), N_2 adsorption–desorption (BET), X-ray Photoelectron Spectroscopy (XPS), Scanning Electron Microscopy (SEM) and Energy Dispersive Spectrometry (EDS). The XRD patterns show that the undoped TiO_2 and co-doped TiO_2 have only anatase form, while the BET surface areas of the co-doped TiO_2 has larger surface area compared to undoped TiO_2. The DRS results indicated that the band gap of co-doped photocatalysts is smaller than undoped TiO_2 and there is a shift in absorption band towards visible light. The SEM images of the co-doped catalysts show the smaller particle size than the undoped catalysts. The photocatalytic efficiency of synthesized catalysts was evaluated by the degradation of methylene blue in solution under visible light irradiation. The degradation results revealed that the co-doped catalysts have better photocatalytic activity than undoped TiO_2 and Degussa P25.

Keywords: Co-doping; methylene blue; sol-gel method; photodegradation;

**Corresponding author: Email: ateshome.abdo225@gmail.com;*

1. INTRODUCTION

Over the last 20 years problems related to hazardous waste remediation have emerged as national and international priority. In order to address this significant environmental problem, different research activities are underway using different advanced analytical, biochemical and physicochemical methods (Hoffmann et al., 1995) for characterization and elimination of hazardous chemicals from air, soil and water. According to literature (Legrini et al., 1993; Robertson, 1996) advanced oxidation process (AOP) is an alternative way of treating undesirable pollutants including dye stuffs. Even though AOP divided in to two categories (heterogeneous and homogenous catalysis), heterogeneous catalysis has been successfully employed for the degradation of various families of hazardous materials (Blake, 2001). Semiconductors used as a catalyst in AOP, in which TiO_2 has been extensively investigated as a heterogeneous photocatalyst for the remediation of contaminated environment (Kim et al. 2005). But it is active only under UV irradiation (λ < 388 nm), since it has a wide band gap energy of about 3.2 eV (Wang et al., 1997) which accounts for less than 4-5% of solar light energy. For a better utilization of the dominant part of the solar spectrum i.e. visible light, the photocatalyst should be made sensitive in visible light. Hence, the search of active photocatalysts in visible light has become a subject of interest for researchers (Jeong et al., 2008). In order to overcome the narrow absorption range of TiO_2, and at the same time to retard possible electron recombination, many groups have been involved in simple doping with transition metal ions (Wang et al. 2008; Yu et al., 2006) or nonmetal elements (Chen et al., 2008) to extend the absorption spectra into the visible region, very few attempts have been made on co-doping of transition metals and nonmetals (Kahan et al., 2008; Sesha et al. 2006; Zhang et al., 2008).

Copper doping has been less explored than the other transition elements and also it appeared from the few literature reports that the doped catalyst has been tested only in the UV-range of radiation (Choi and Kang, 2007). The sol-gel preparation of alkaline earth metal (magnesium) doped nano TiO_2 is not widely reported (Venkatachalam et al., 2007), even if it is more abundant element and less hazardous to use. The co-doped nanocatalysts of TiO_2 with a combination of alkaline earth metal and transition metal ions are not reported so far. So, authors are interested in the preparation of new catalyst by co-doping of magnesium(II) and copper(II) into TiO_2 matrix. The ionic radii of both Mg^{2+} (0.72 A^0) and Cu^{2+} (0.73 A^0) are closer to that of Ti^{4+} (0.68 A^0) (Shannon, 1976) to incorporate them easily into TiO_2 matrix. The photocatalytic activities of catalysts were evaluated by the degradation of methylene blue as representative dye pollutant. The effect of dopant concentration pH, catalyst dosage and dye concentration on the photocatalytic activity of prepared catalysts have been examined in detail.

2. EXPERIMENTAL DETAILS

2.1 Catalyst Preparation

All the starting materials were reagent grade and were used without further purification and double distilled water was used for solutions preparation. Titanium tetra-n-butoxide ($Ti(O\text{-}Bu)_4$) and nitrates of magnesium and copper metals are obtained from E- Merck (Germany) were used as titanium, magnesium and copper sources for preparing undoped TiO_2 and co-doped TiO_2 catalysts respectively. Methylene blue dye was used as a model compound for

degradation. A sol-gel method (Zhang et al., 2008) was employed to prepare co-doped TiO_2 catalysts.

2.1.1 Procedure

Initially a solution containing 20 mL of absolute alcohol, 3 mL of H_2O, and metal nitrates for Mg^{2+} 0.07793 g – 0.3173 g and for Cu^{2+} 0.0281 g to 0.11234 g are taken for the preparation of required percentages (solution-I). Another solution (solution-II) was prepared using 10.5 mL of $Ti(O\text{-}Bu)_4$ dissolved in 20 mL of absolute alcohol with stirring for 10 minutes, and then 1.5 mL of HNO_3 was added drop wise under continuous stirring for 30 minutes. Solution-I was added to solution-II slowly from the burette with vigorous stirring at room temperature until the transparent sol was obtained, and the resulting sol was further stirred for 1h. The gel was prepared by aging the sol for 48 h at room temperature. The derived gel was dried at 100 ^{0}C in an oven and ground. The catalyst powder was calcined at 400 ^{0}C in furnace for 2 h. Undoped TiO_2 is also prepared with same procedure without metal nitrates. Figure 1 illustrates the pattern of sol-gel method.

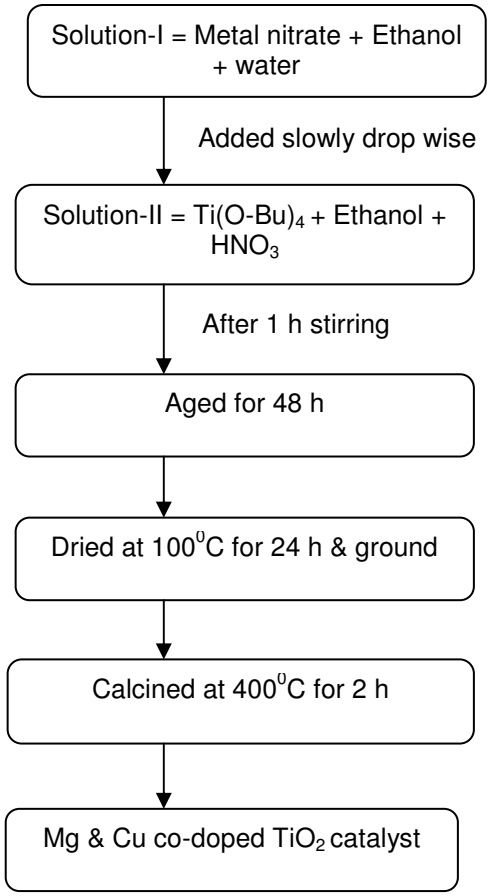

Fig. 1. Schematic diagram of the sol-gel method for the preparation of the catalyst.

2.2 Characterization of Catalysts

The Diffuse reflectance spectra (DRS) were recorded with a Shimadzu 3600 UV-Visible NIR spectrophotometer equipped with an integrating sphere diffuse reflectance accessory, using $BaSO_4$ as reference scatter. Powder samples were loaded into a quartz cell and spectra were recorded in the range of 200-900 nm. Crystalline structures of photocatalysts were determined by X-ray diffractometer (Model Ultima IV, RIGAKU) using CuKα (λ =0.154059 nm) radiation with a nickel filter. The applied current and voltage were 40 mA and 40 kV, respectively. The 2θ scanning range was 3^0 to 90^0 with a scan rate of 2^0 min^{-1}. The Brunauer-Emmett-Teller (BET) surface area was determined from the N_2 adsorption-desorption isotherm at 77.3 K by using a Quantachrome Nova 2200 E system. The sample was out gassed for 3 h at 300 ^{0}C prior to the adsorption. The specific surface area was determined by using the standard BET method. X-ray photoelectron spectroscopy (XPS) was recorded with a PHI quantum ESCA microprobe system, using the AlKα line of a 250 W X-ray tube as a radiation source with the energy of 1253.6 eV, 16 mA × 12.5 kV and a working pressure lower than 1×10^{-8} Nm^{-2}. As an internal reference for the absolute binding energies, the C 1*s* peak of hydrocarbon contamination was used as reference to 284.8 eV. The fitting of XPS curves was analyzed with Multipak 6.0 A software. The morphology and size of particles was characterized using scanning electron microscope (SEM) (JSM-6610 LV) equipped with an energy dispersive X-ray (EDS) spectrophotometer and operated at 20kV.

2.3 Photo Activity Measurements

The high pressure mercury vapor lamp (400W, Osoram) with UV filter has been used as a visible light source (output is 436 - 546 nm) with 35000 lumen and placed 20 cm away from the photo reactor. The photoreactor setup has been given elsewhere (Jeffrey, 2004). Cut off filter was placed in the path of light for complete removal of UV radiation and running water was circulated around the sample container to filter IR radiation and to keep the reaction mixture at room temperature.

A general photocatalytic procedure was carried out with a required amount of catalyst added to fresh 100 mL aqueous dye solution of required concentration in 150 ml Pyrex glass vessel with continues stirring. Prior to irradiation the solution with catalyst was stirred in the dark for 45 minutes to ensure establishment of adsorption–desorption equilibrium of MB dye on catalyst surface. Aliquots of the samples were withdrawn from the solution by using Millipore syringe (0.45 µm) at certain time intervals and analyzed for methylene blue dye concentration. The percentage degradation of dye was checked by measuring the absorbance of dye solution at 660 nm using a UV–visible (Milton-Roy Spectronic 1201) Spectrophotometer. A pH meter (Digital pH meter model 111E, EI) was used for adjusting and investigation of pH variation during the process. The pH of the dye solutions was adjusted prior to irradiation by addition of 0.1N NaOH or 0.1N HCl to get required pH.

3. RESULTS AND DISCUSSION

3.1 Diffuse Reflectance Spectra

The diffuse reflectance spectra (DRS) of the co-doped and undoped TiO_2 samples are given in Fig. 2. The spectra of undoped TiO_2 showed an absorption peak at 388 nm in the UV region (Anpo and Takeuchi, 2003). There are bands in the region of 220-260 nm of Fig. 2,

which show O^{2-} (2p) ⟶ Cu^{2+} (3d) ligand to metal charge transfer. This result is in good agreement with reported by (Colon et al. 2006). The co-doped TiO_2 with different percentages of Mg^{2+} & Cu^{2+} has shown considerable shift in the absorption peak towards the visible region at around 400-900 nm for all the samples. The tailing absorption peaks can be considered as the extra tail states in the band gap because of the synergistic effect of added Mg^{2+} & Cu^{2+} to the TiO_2 matrix (Forsh et al. 2001). The extension of adsorption edge to longer wave lengths for Mg^{2+} & Cu^{2+}/TiO_2 indicates the existence of good contact between TiO_2 and Mg & Cu grains and promotes the photocatalytic activity of catalysts in visible light.

The UV-vis. absorption edge and band gap energies of the samples have been determined from the reflectance [F(R)] spectra using the Kubelka-Monk (KM) formalism and Tauc plot (Yoong et al. 2009). For the semiconductor materials, a plot of $[F(R).h\nu]^n$ against $h\nu$ should show a linear region just above the optical absorption edge for n = ½ if the band gap is direct transition, or for n = 2 if it is indirect (Murphy, 2007) over the linear region of plots, the relationship has been given elsewhere (Yoong et al. 2009). The extrapolated line shown in Fig. 3, have been used to determine the band gap energy for different Mg(II) & Cu(II) co-doped TiO_2 and undoped TiO_2 samples. The calculated band gap energies are given in Table 1. The largest reduction band gap is observed for co-doped catalysts of 0.75 wt % of Mg & 0.25 wt % of Cu and 0.50 wt % of Mg & 0.50 wt % of Cu co-doped TiO_2. This large reduction band gap may be attributed to those impurities incorporated into the host (TiO_2) structure which create extra energy levels within the band gap (Thomas and Thomas, 1997). Due to the creation of extra energy level with in the band gap, Fermi energy will shift away from the centre of the band gap towards valence band since both metals create P-type semiconductor.

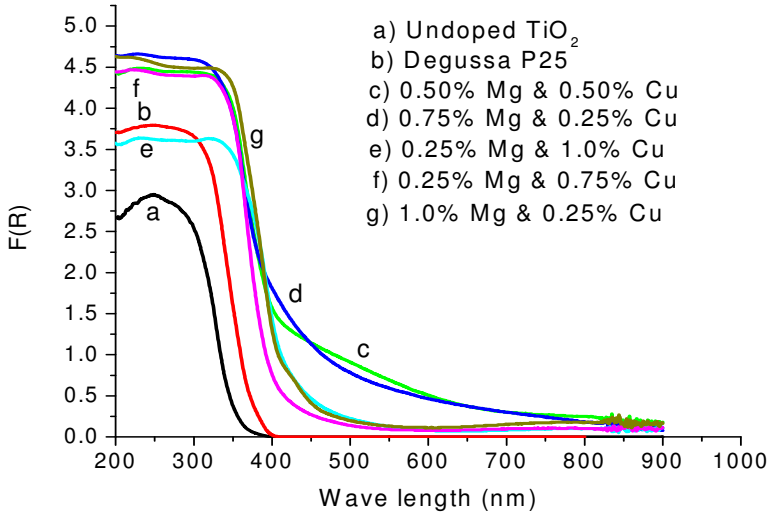

Fig. 2. The DRS -UV-vis. spectra of co-doped TiO_2 with different percentage of Mg & Cu and Degussa P25

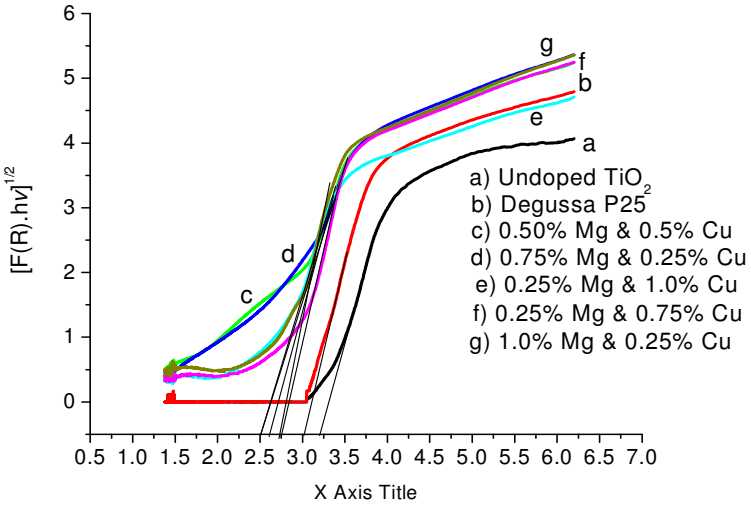

Fig. 3. Plots of transformed Kubelka-Munk functions $[F(R).h\nu]^{1/2}$ versus hν for different percentage of co-doped TiO_2, undoped TiO_2 and Degussa P25 samples

3.2 X-Ray Diffraction Study and BET Results

A series of a) 0.25 wt % of Mg & 1.0 wt % of Cu, b) 0.75 wt % of Mg & 0.25 wt % of Cu, c) 0.50 wt % of Mg & 0.50 wt % of Cu, Mg & Cu co-doped TiO_2 samples and d) undoped TiO_2 nano crystalline titania were successfully prepared and characterized by XRD. The XRD patterns of undoped TiO_2 and co-doped TiO_2 powder samples were given in Fig. 4. All the peaks in the XRD patterns correspond to the reported data of anatase TiO_2 (JCPDS, 00-021-1272, JCPDS, 01-086-1157). Since the ionic radii of Mg^{2+} (0.72 A^0) and Cu^{2+} (0.73 A^0) are closer to that of Ti^{4+} (0.68 A^0) it is easier for these ions to be incorporated into the matrix of TiO_2 without causing much crystalline distortion. The average particle size of prepared catalysts was calculated from the broadening of the full width at half maximum (FWHM) peak (1 0 1) using Scherrer's equation (Jeong et al., 2008) ranges from 10 to 39.96 nm. The doped TiO_2 did not show the presence of magnesium or copper related oxide. The BET surface area results have shown that there is a much increase in surface area of co-doped catalysts than undoped and Degussa P 25. With the incorporation of Cu^{2+} and Mg^{2+} dopants during the sol-gel preparation technique there was crystal growth suppression, favoring the formation of smaller TiO_2 crystallite. This effect may be attributed to the enhanced lattice strain in the doped TiO_2 network and then decrease grain growth rate. Similar observation was reported by Yang et al. (Yang et al., 2009). Furthermore, this higher surface area values also may be due to the removal of nitrate from the crystal during calcinations at temperature lower than 400 ^{0}C which is from Cu and Mg (magnesium and copper nitrates) precursors and thermally decompose. This will increase the porosity of surface which results in increasing surface area of the doped TiO_2 than undoped one as also reported by (Colon et al., 2006). This result is also given in Table 1.

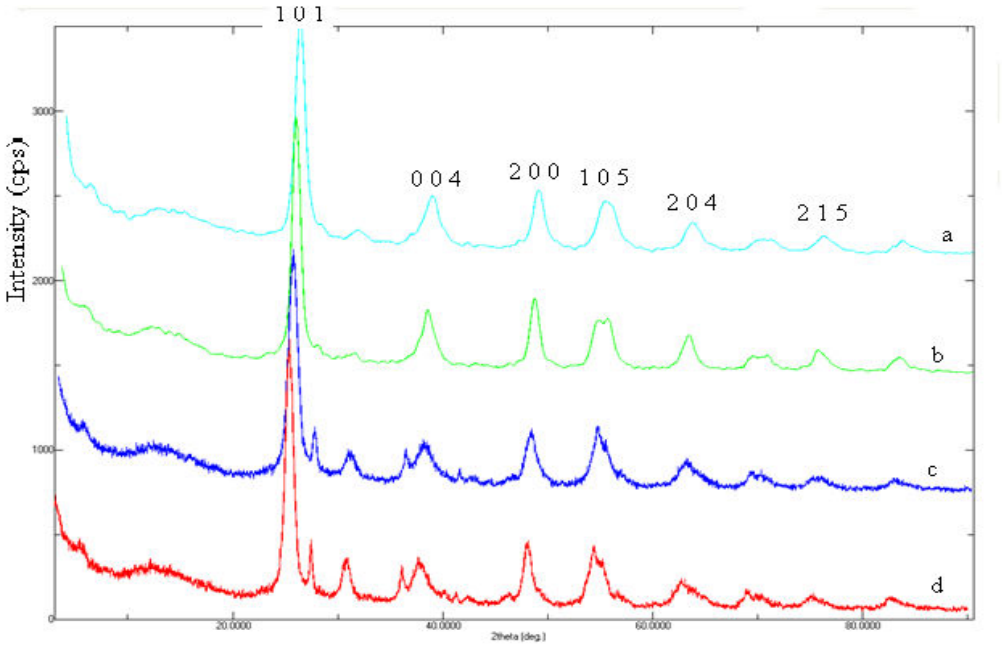

Fig. 4. XRD patterns of (a) 0.25 wt % of Mg & 1.0 wt % of Cu co-doped TiO_2, (b) 0.75 wt % of Mg & 0.25 wt % of Cu co-doped TiO_2, (c) 0.50 wt % of Mg & 0.50 wt % of Cu co-doped TiO_2 and (d) Undoped TiO_2

Table 1. BET surface area and Band gap energy of each catalyst, calcined at 400^0C

Sample No.	Photocatalyst	Crystallite size (nm)	BET surface area (m^2/g),	Band gap energy (eV), from DRS spectra
1	0.25 wt % Mg & 1.0 wt % Cu	12.04	88.442	2.60
2	0.25 wt % Mg & 0.75 wt % Cu	13.14	84.342	2.75
3	0.75 wt % Mg & 0.25 wt % Cu	10.00	111.713	2.50
4	1.0 wt % Mg & 0.25 wt % Cu	39.96	98.907	2.8
5	0.50 wt % Mg & 0.50 wt % Cu	10.13	100.486	2.50
6	Undoped TiO_2	16.50	79.382	3.2
7	Degussa P25	-	69.962	3.1

Based on the trial photodegradation of MB with above samples, samples 3 and sample 5 have shown higher degradation rate. Hence, the further characterizations have been done only for these two samples.

3.3 X-Ray Photoelectron Spectroscopy

X-ray photoelectron spectroscopy (XPS) analysis of copper(II) and magnesium(II) co-doped sample was performed, and the survey spectrum and high-resolution scans are shown in Figure 5. From the XPS survey spectrum of Cu, Mg, Ti and O photoelectron lines were detected along with C peaks. The XPS observations were consistent with EDS results in that, only Cu, Mg, Ti and O, elements were detected from the samples in survey spectrum analysis. In Fig. 5 (b), Cu $2p_{3/2}$ and Cu $2p_{1/2}$ peaks were located at binding energies of 934.400 and 954.209 eV respectively, and were belongs to the compound of CuO (Tseng et al., 2004; Xu et al., 2010) and shake-up peaks are also observed which is a characteristics for Cu^{2+} that bonds with oxygen atoms. The binding energy of Mg 2p was found to be 50.967 eV which is a typical of Mg^{2+} that bonded to oxygen and it was assigned to the compound MgO (Moulder et al., 1992). The binding energies of Ti $2p_{3/2}$ and Ti $2p_{1/2}$ were found to be 458.493 and 464.012 eV and these bands could be belongs to Ti^{4+} (Choi and Kang, 2007) and there was no fitting peak for Ti^{3+}. Hence the XPS spectra confirmed the chemical composition of magnesium and copper co-doped sample to be CuO, MgO and TiO_2.

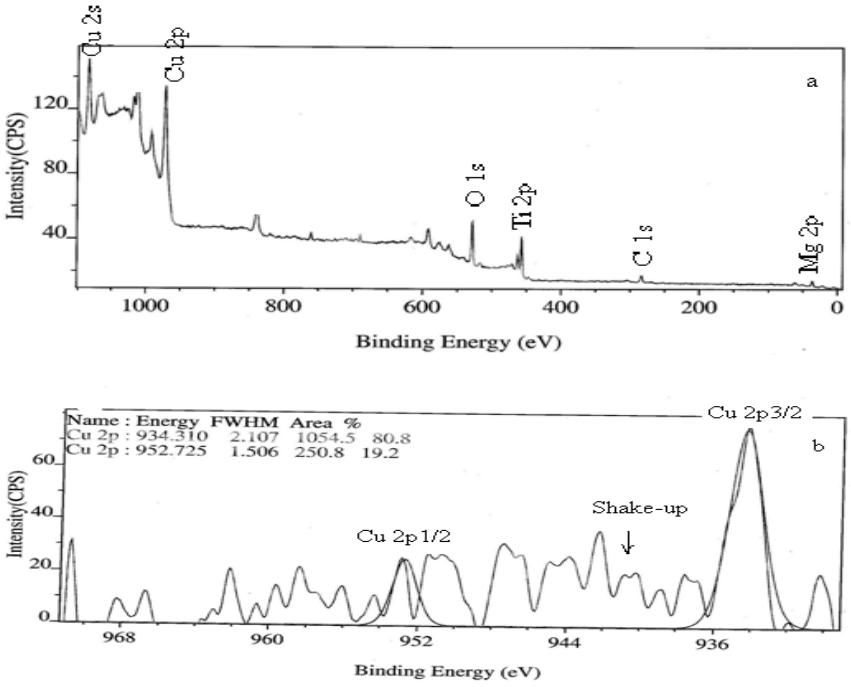

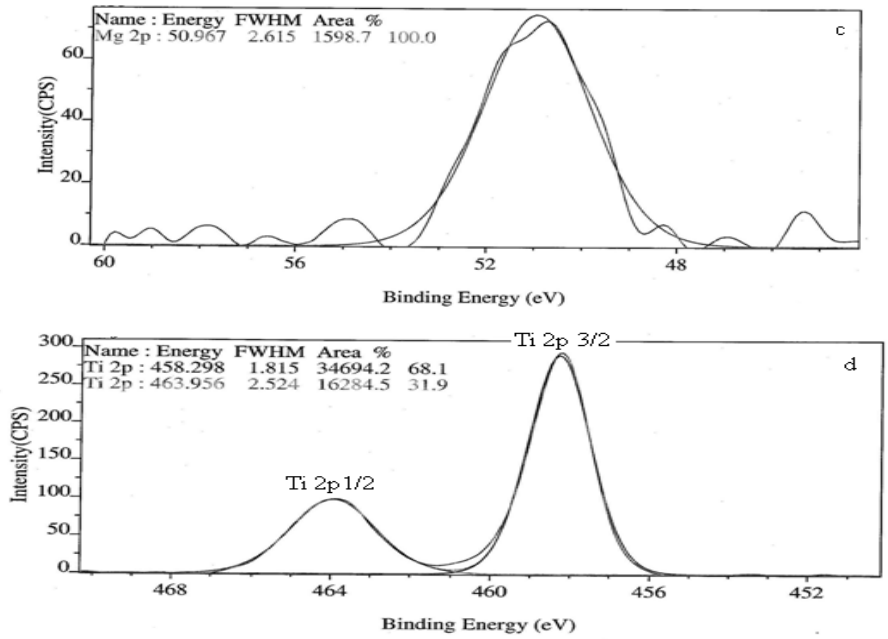

Fig. 5. (a) XPS survey spectrum of magnesium & copper co-doped TiO_2 (b) High resolution of Cu 2p spectrum (c) High resolution of Mg 2p and (d) High resolution of Ti 2p spectrum

3.4 Scanning Electron Microscopy and Energy Dispersive Spectrometry

3.4.1 Scanning electron microscopy

The SEM images of undoped and co-doped TiO_2 (sample 3 & 5) is shown in Figure 6. There is uneven distribution of agglomerated particles. However, they generally consisted of spherical particles and many micro and mesopores were expected at the interstices of the particles, and also they show the morphological changes with an average particle size of 1.2 µm, 0.64 µm and 0.95µm respectively. The decrease in particle size and increase in surface area of catalyst shows an enhanced photocatalytic activity.

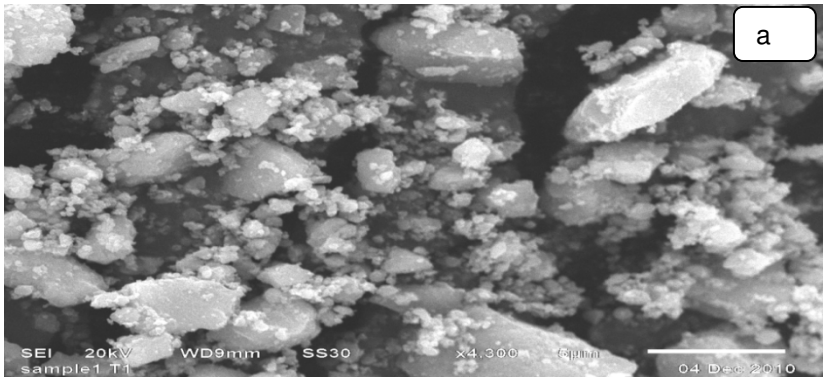

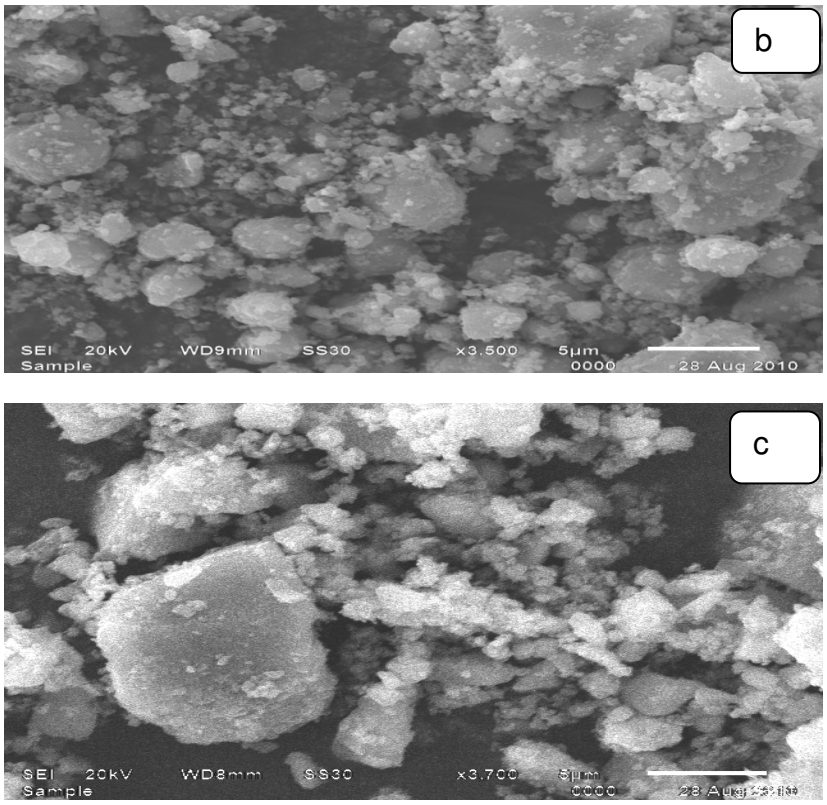

Fig. 6. SEM images of (a) Undoped TiO_2 (b) Co-doped TiO_2 with 0.75 wt % of Mg & 0.25 wt % of Cu and (c) 0.50 wt % of Mg & 0.50 wt % of Cu.

3.4.2 Energy dispersive spectrometry

The energy dispersive spectrometry (EDS) used to identify elements exist in the prepared catalyst by taking a selective portion of SEM image in the form of peaks of spectrum. The elemental composition of the prepared catalysts are listed in the Table 2a & b in percentage weight as well as percentage of atomic elements in the sample and its spectral images are given in Figures 7a & b.

Table 2a. Composition of the 0.75 wt% of Mg & 0.25 wt% of Cu co-doped TiO_2 catalyst

Element	Weight%	Atomic%	Compd%	Formula
Mg	0.76	0.49	0.74	MgO
Ti	59.20	32.93	98.91	TiO_2
Cu	0.24	0.12	0.35	CuO
O	39.80	66.47		
Totals	100.00			

Table 2b. Composition of the 0.50 wt% of Mg & 0.50 wt% of Cu co-doped TiO_2 catalyst

Element	Weight%	Atomic%	Compd%	Formula
Mg	0.53	0.62	0.94	MgO
Ti	59.06	32.80	98.51	TiO_2
Cu	0.47	0.19	0.55	CuO
O	39.94	66.40		
Totals	100.00			

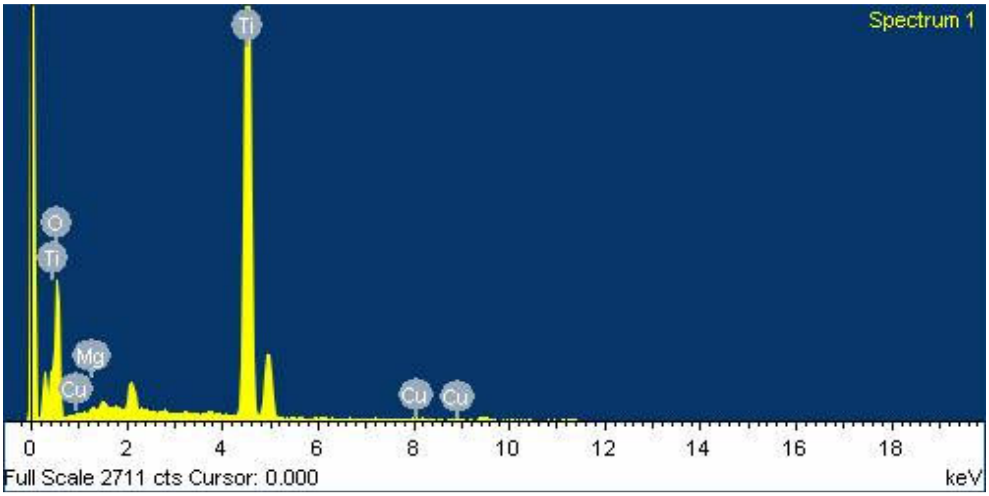

Fig. 7a. EDS spectrum of 0.75 wt% of Mg & 0.25 wt% of Cu co-doped TiO_2.

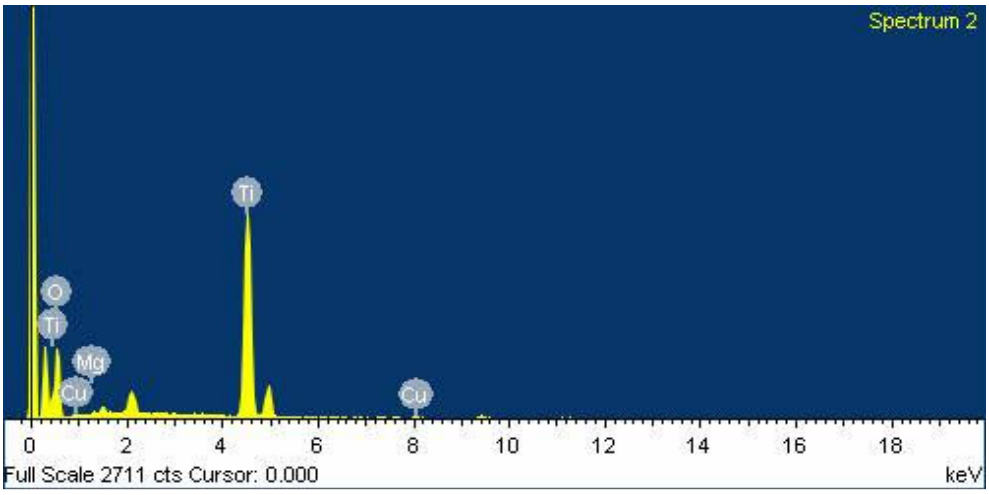

Fig. 7b. EDS spectrum of 0.50 wt % of Mg & 0.50 wt% of Cu co-doped TiO_2

The possible formulae of compounds in the prepared catalysts were also found from EDS analysis presented in the Table. Hence, this analysis confirms the presence of both magnesium and copper in the TiO_2 matrix.

3.5 Photocatalytic Activity of Catalyst - Degradation of Methylene Blue

In a controlled experiment, 50.0 mL of 10 ppm solution containing methylene blue was taken in four beakers. The first beaker was kept in dark and the second beaker was in light for 4 h. The third and fourth beakers containing dye and 0.10 g of catalyst were kept in dark and exposed to visible light for 4 h respectively. The absorbance of the MB solution of four beakers was measured by spectrophotometer. It was observed that solutions of the first three beakers has no significant change in initial absorbance, while the absorbance of solution in the fourth beaker has shown drastic decrease from initial absorbance, indicating that the degradation reaction is a photocatalytic reaction in which both catalysts and visible light are required for the reaction to proceed. The result was in good agreement with the previous report by (Mohamed and Al-Esaimi 2006). Experimental parameters like concentration of dopants, catalyst dosage, pH of the solution and initial concentration of pollutant would affect the efficiency of co-doped nanocatalyst. Hence, it is critical to optimize these parameters to achieve higher degradation efficiency of photocatalyts for degradation of methylene blue.

3.5.1 Effect of dopant concentration on the degradation of MB

To determine the optimum dopant concentration of the co-doped TiO_2, experiments were carried out with catalysts for the degradation of methylene blue under visible light irradiations. The rate of degradation of MB has been quantified by the measurement of MB absorbance and the results are presented in Fig. 8. It can be observed from the figure that the photocatalytic performance of TiO_2 was higher by co-doping with Mg and Cu at 0.75 & 0.25 wt % and 0.50 & 0.50 wt %. The highest photocatalytic performance of the co-doped catalyst may be because of its high surface area (Table 1). Furthermore figure 8 show that the co-doped catalysts display higher catalytic activity than Mg and Cu single doped TiO_2. Similar results has been reported by (Deng et al., 2009) that V and Ga co-doping rather than sole V or Ga doping can alter the band gap of TiO_2 significantly and they also observed the content and the proportion of V and Ga play dominant role for narrowing the band gap of TiO_2.

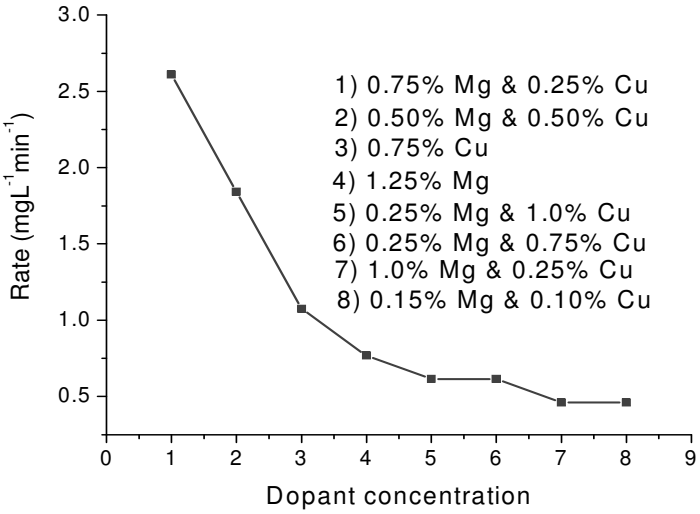

Fig. 8. Effect of dopant concentration on the rate of degradation of methylene blue. Catalyst Dosage = 0.10g, pH = 9 and [MB] = 10 ppm.

3.5.2 Effect of solution pH

The influence of pH on the degradation of MB is shown in Figure 9. The results showed that there was a strong dependence of the heterogeneous photoprocess on pH of the solution. It is known that the metal oxide particles suspended in water behave similar to diprotic acids. For TiO_2, hydroxyl groups undergo two acid base equilibria (Saquib et al., 2008; Senthilkumaar et al. 2006):

$$>TiOH_2^+ \rightleftharpoons >TiOH + H^+, \quad pH < 6.25$$

$$>TiO^- + H^+ \rightleftharpoons >TiOH, \quad pH > 6.25$$

Tang and An (1995) and Wang et al. (2000) showed that for charged substrates, there is a significant dependency of the photocatalytic degradation efficiency on pH value, since the overall surface charge and hence the adsorptive properties of TiO_2 particles depend strongly on solution pH.

In this experiment, any change in rate of degradation with varying pH values can be related to variations of the acid/base properties of the Mg^{2+} & Cu^{2+} co-doped TiO_2 particle surface. The MB is a cationic dye in aqueous solution and in an acidic pH the surface of catalyst (Mg^{2+} & Cu^{2+} co-doped TiO_2) and MB dye will both attain positive charge and there would be electrostatic repulsion between them, which retards the degradation percentage of the dye. But in basic pH since MB is cationic dye in aqueous solution and the surface of the catalyst attains negative charge, there would be electrostatic attraction which would enhance

degradation percentage and it reach maximum at pH 10. In alkaline pH values, there would be a chance for hydroxyl radicals to diffuse away and degrade the dye in the bulk solution (Saquib et al., 2008). (Poulios and Tsachpinis, 1999) previously reported similar behavior on the photodegradation of other cationic dyes.

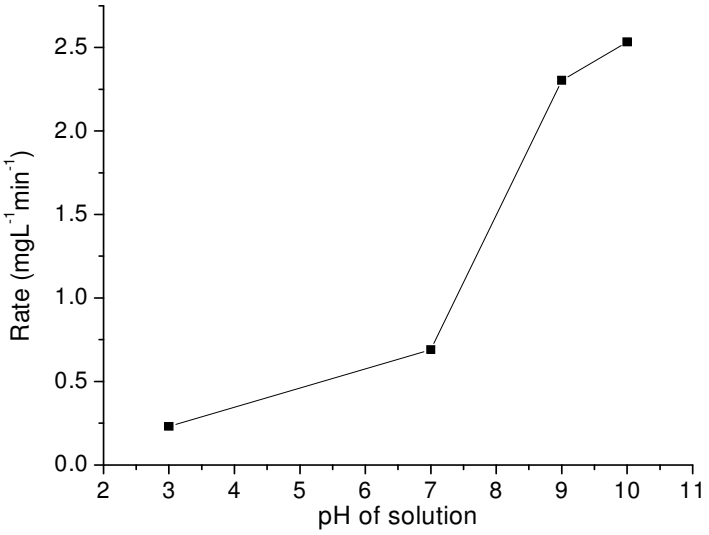

Fig. 9. The effect of pH on the rate of degradation of methylene blue by Mg^{2+} and Cu^{2+} co-doped TiO_2. Catalyst dosage = 0.10 g and [MB] = 10 ppm

3.5.3 Effect of catalyst dosage

A series of experiments were conducted to study the effect of catalyst dosage on the degradation of methylene blue and to get optimum catalyst loading by varying the nano co-doped TiO_2 from 0.025 to 0.3 g in 100 mL methylene blue solution of concentration 10 ppm. The rate of degradation increases with increase of catalyst loading up to 0.1 g since the number of photons absorbed and the number of dye molecules adsorbed are increased with respect to an increase in the number of catalyst molecules until the active surface becomes constant. After certain number of catalyst molecules, the dye molecules are not sufficient for adsorption by increased number of catalyst molecules. Hence the additional catalyst powder is not effectively involved in the photocatalytic activity rather increase in the turbidity of the solution, which interfere with penetration of light transmission. Further, it was explained that the deactivation of activated molecule by collision with the ground state molecule with the shielding of TiO_2 may also take place (Chen, 2007; Neppolian et al. 2002; Sahoo et al., 2005; Saritha et al., 2007; Sauer et al., 2002). The effect of catalyst dose is given in Figure 10.

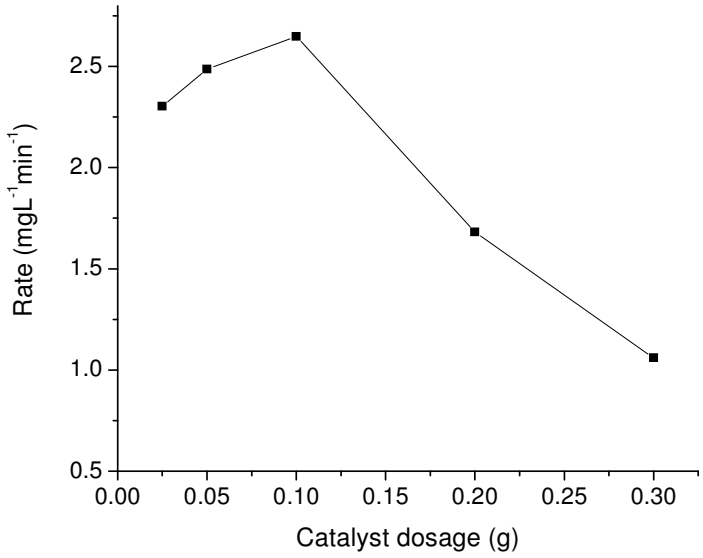

Fig. 10. The effect of catalyst dosage on the rate of degradation of methylene blue by Mg^{2+}/Cu^{2+} co-doped TiO_2, pH = 10 and [MB] = 10 ppm.

3.5.4 Effect of methylene blue initial concentration

The effect of initial methylene blue concentration on rate of degradation of the dye is illustrated in Figure 11.

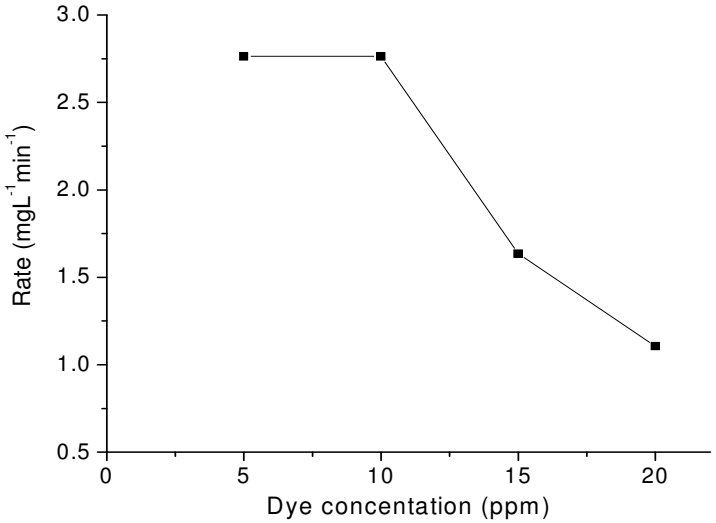

Fig. 11. The effect of initial concentration of dye on the rate of degradation of methylene blue pH = 10, catalyst dosage = 0.10 g.

The influence of initial concentration of methylene blue on rate of degradation was studied from 5 ppm to 20 ppm at a fixed concentration of catalyst (0.10 g of 0.75 wt % of Mg & 0.25 wt % of Cu co-doped TiO_2), using a solution of pH 10 of 100 mL methylene blue in 150 ml Pyrex glass. Photocatalytic degradation increases with increase in the concentration of dye up to 10 ppm. This may be attributed to the fact that as the concentration of the dye increased, more dye molecules will be available for excitation and energy transfer (Balaram et al. 2010; Poulios and Tsachpinis, 1999), which increases the percentage of degradation. But beyond 10 ppm of the dye concentration it may adversely affect the percentage of degradation (Kusvuran et al., 2004). This is due to the fact that at higher concentration dyes start covering the surface of photocatalyst from light intensity.

At dopant concentration of 0.75 wt.% of Mg^{2+} & 0.25 wt.% of Cu^{2+} co-doped TiO_2, pH 10, catalyst dosage 0.10 g and when the 10 ppm MB is the initial concentration, the rate of degradation is high when compared with the previous works (Ge et al., 2006; Shi et al., 2011; Wang et al., 2009). The rate constant of degradation of MB with best catalyst so prepared was estimated from the slope of percentage degradation versus time to be 8.33 X 10^{-3} min^{-1}.

3.6 Photocatalytic Mechanism

Based on the experimental results the following mechanism would be proposed for the photocatalytic reactions of magnesium and copper co-doped TiO_2 (Balaram et al., 2010; Saquib et al., 2008; Senthilkumaar et al., 2006; Venkatachalam et al., 2007).

a. Upon visible light illumination of photocatalyst, electrons are ejected from the valence band to the conduction band leaving positive holes in the valence band.

$$TiO_2 + hv \longrightarrow h^+_{vb} + e^-_{cb}$$

b. The metal ions co-doped into TiO_2 lattice, trapped these ejected electrons, holding up the recombination process.

$$\left.\begin{aligned} Cu^{2+} + e^- &\longrightarrow Cu^+ \\ Mg^{2+} + e^- &\longrightarrow Mg^+ \end{aligned}\right\} \text{Un-stable}$$

c. The trapped electrons can be further scavenged by molecular oxygen, which is adsorbed on the TiO_2 surface, to generate superoxide radical, and this in turn produces hydrogen peroxide (H_2O_2), hydroperoxy (HO_2 •) and hydroxyl (•OH) radicals.

$$Cu^+ + O_2 \longrightarrow Cu^{2+} + O_2^{\bullet -}$$

$$Mg^+ + O_2 \longrightarrow Mg^{2+} + O_2^{\bullet -}$$

$$O_2^{\bullet -} + H_2O \longrightarrow HO_2^{\bullet} + OH^-$$

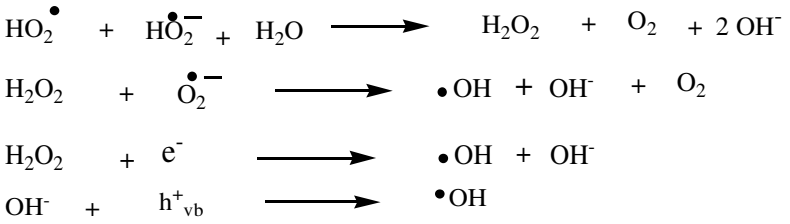

d. The positive holes in the valence band act as good oxidizing agents available for degradation of dye in the solution, •OH (or h^+) where 'dye' is the pollutant, an electron donor.

Thus, the MB is attacked by the hydroxyl radicals formed both by trapped electrons and hole in the VB as given in the above equations, to generate organic radicals or other intermediates, which further undergo degradation.

4. CONCLUSION

The DRS analysis show that co-doping of Mg^{2+}/Cu^{2+} into TiO_2 shifts the absorbance band of TiO_2 from UV to visible region and the band gap energy is reduced for all co-doped catalysts (from 3.2 eV to 2.50 eV), the largest reduction gap was observed for co-doped catalysts of 0.75 wt. % of Mg & 0.25 wt. % of Cu. The incorporation of Mg^{2+} and Cu^{2+} ions into the TiO_2 were evidenced by XPS analysis and EDS results. The BET results also show that there is an increase in surface area of the catalyst, which enhances the photocatalytic degradation of methylene blue in visible light. The photocatalytic degradation of methylene blue over the catalyst surface of nano co-doped Mg^{2+} / Cu^{2+} TiO_2 is higher than over undoped TiO_2 and Degussa P25. The enhanced adsorption of methylene blue over the catalyst surface is increased by increasing pH.

ACKNOWLEDGEMENTS

One of the authors Teshome Abdo Segne gratefully acknowledges the financial support from the Government of The Federal Democratic Republic of Ethiopia, Addis Ababa, through Embassy of the Federal Democratic Republic of Ethiopia, New Delhi (India).

REFERENCES

Anpo, M., Takeuchi, M. (2003). The design and development of highly reactive titanium oxide photocatalysts operating under visible light irradiation. J. Catal., 216, 505-516.

Balaram, K.A., Siva, R.T., Sreedhar, B. (2010). Synthesis, characterization and photocatalytic activity of alkaline earth metal doped titania. Ind. J. Chem., 49, 1189-1196.

Blake, D. (2001). Bibliography of work on the heterogeneous photocataloytic removal of hazardous compounds from water and air, NREL/TP-510-31319) NTIS. U.S. Dept. of Commerce, Spring field.

Chen, C.C. (2007). Degradation pathways of ethyl violet by photocatalytic reaction with ZnO dispersions. J. Molecular Catalysis A: Chemical, 264, 82-92.

Chen, X., Glans, P.A., Qiu, X., Dayal, S., Jennings, W.D., Smith, K.E., Burda C., Guo, J. (2008). X- ray spectroscopic study of the electronic structure of visible-light responsive N-, C- and S-doped TiO_2. J. Electron Spectrosc. Relat. Phenom., 162, 67–73.

Choi, H. J., Kang, M. (2007). Hydrogen production from methanol/water decomposition in a liquid photosystem using the anatase structure of Cu loaded TiO_2. Int. J. Hydrog. Energy., 32, 3841-3848.

Colon, G., Maicu, M., Hidalgo M.C., Navio, J.A. (2006). Cu-doped TiO_2 system with improved photocatalytic activity. Appl. Catal. B Environ., 67, 41-51.

Deng, Q.R., Gao, Y., Xia, X.H., Chen, R.S., Wan, L., Shoa, G. (2009). V and Ga co-doping effect on optical absorption properties of TiO_2 thin films, J. Physics: conference Series, 152, 012073.

Forsh, P.A., Kazanskii, A.G., Mell H., Terukov, E.I. (2001). Photoelectrical properties of microcrystalline silicon films, Thin Solid Films., 383, 251-253.

Ge, L., Xu, M., Fang, H. (2006). Photocatalytic degradation of methyl orange and formaldehyde by Ag/InVO4-TiO2 thin films under visible light irradiation. J. Molecular Catalysis A: Chemical, 238, 68-76.

Hoffmann, M.R., Martin, S.T., Choi W., Bahnemann, D.W. (1995). Environmental applications of semiconductor photocatalysis. Chem. Rev., 95, 69-95.

JCPDS Reference Code: 00-021-1272.

JCPDS Reference Code: 01-086-1157.

Jeffrey, C., Wu S., Chen, C.H. (2004). A visible-light response vanadium-doped titania nanocatalyst by sol–gel method, J. Photochemistry and Photobiology A: Chem., 163, 509-515.

Jeong, E.D., Borse, P.H., Jang, J.S., Lee, J.S., Ok-Sang Jung, Chang, H., Jin, J.S., Won, M.S., Kim, H.G. (2008). Hydrothermal synthesis of Cr and Fe co-doped TiO_2 nanoparticle photocatalyst. J. Ceramic Processing Res., 9, 250-253.

Kahan, R., Kim, S.W., Kim T.J., Nam, C.M. (2008). Comparative study of the photocatalytic performance of boron-iron co-doped and boron-doped TiO_2 nanoparticles. Material Chem. Phys., 112, 167-172.

Kim, S., Hwang S.J., Choi, W. (2005). Visible light active platinum-ion-doped TiO_2 photocatlyst. J. Phys. Chem. B., 109, 24260-24267.

Kusvuran, E., Gulnaz, O., Irmak, S., Atanur, O.M., Yavuz, H.I., Erbatur, O. (2004). Comparison of several advanced oxidation processes for the decolorization of Reactive Red 120 azo dye in aqueous solution. J. Hazardous Materials B., 109, 85-93.

Legrini, O., Oliveros, E., Braun, A.M. (1993). Photochemical processes for water treatment. Chem. Rev., 93, 671-698.

Mohamed, M.M., Al-Esaimi, M.M. (2006). Characterization, adsorption and photocatalytic activity of vanadium-doped TiO_2 and sulfated TiO_2 (rutile) catalysts: Degradation of methylene blue dye. J. Molecular Catalysis A: Chemical., 255, 53-61.

Moulder, J.F., Stickle, F.W., Sobol, P.E., Bomben, K. D. (1992). Handbook of X-ray Photoelectron Spectroscopy, (Perkin-Elmer, Eden Prairie, MN).

Murphy, A.B. (2007). Band-gap determination from diffuse reflectance measurement of semiconductor films, and application to photoelectrochemical water-splitting. J. Sol. Energ. Mat. Sol. C., 91, 1326-1337.

Neppolian, B., Sakthivel, S., Palanichamy, M., Arabindoo, B., Murugasen, V. (2002). Solar/UV induced photocatalytic degradation of three commercial textile dyes. J. Hazard Mater B., 89, 303-317.

Poulios, I., Tsachpinis, I. (1999). Photodegradation of the textile dye reactive black 5 in the presence of semiconducting oxides. J. Chem. Technol Biotechnol., 71, 349-357.

Robertson, P.K.J. (1996). Semiconductor photocatalysis: an environmentally acceptable alternative production technique and effluent treatment process. J. Cleaner Prod., 4, 203-212.

Sahoo, C., Gupta, A.K., Pal, A. (2005). Photocatalytic degradation of Crystal Violet (C.I. Basic Violet 3) on silver ion doped TiO_2. Dyes and Pigments, 66, 189-196.

Saquib, M., Abu Tariq, M., Faisal, M., Muneer, M. (2008). Photocatalytic degradation of two selected dye derivatives in aqueous suspensions of titanium dioxide. J. Desalination, 219, 301-311.

Saritha, P., Aparna, C., Anjaneyulu, V.H. (2007). Comparison of various advanced oxidation processes for the degradation of 4-chloro-2 nitrophenol. J. Hazardous Materials, 149, 609-614.

Sauer, T., Neto, G.C., Jose, H.J., Moreira, R.F.P.M. (2002). Kinetics of photocatalytic degradation of reactive dyes in a TiO_2 slurry reactor. J. Photochem. Photobiol. A, 149, 147-154.

Senthilkumaar, S., Porkodi, K., Gomathi, R., Geetha, A.M., Manonmani, N. (2006). Sol-gel derived silver doped nanocrystalline titania catalysed photodegradation of methylene blue from aqueous solution. J. Dyes Pigments, 69, 22-30.

Sesha, S., Sirinivasan, J.W., Elias K.S., Yogi, G. (2006). Synergistic effect of sulfation and co- doping on visible light photocatalysis of TiO_2. J. Alloys Compounds., 424, 322-326.

Shannon, R.D. (1976). Revised effective ionic radii and systematic studies of interatomic distances in halides and chalcogenides. Acta Cryt. A, 32, 751-767.

Shi, Z., Zhang, X., Yao, S. (2011). Preparation and photocatalytic activity of TiO_2 nanoparticles co-doped with Fe and La, Particuology.

Tang, W.Z., An, H. (1995). UV/TiO_2 photocatalytic oxidation of commercial dyes in aqueous solutions. Chemosphere, 31, 4157-4170.

Thomas, M., Thomas, W.J. (1997). Principles and Practice of Heterogeneous Catalysis. CH Publishers Inc., New York, NY (USA).

Tseng, I.H., Wu, J.C.S., Chou, H.Y. (2004). Effects of sol-gel procedures on the photocatalysis of Cu/TiO_2 in CO_2 photoreduction. J Catal., 221, 432-440.

Venkatachalam, N., Palanichamy, M., Murugesan, V. (2007). Sol–gel preparation and characterization of alkaline earth metal doped nano TiO_2: Efficient photocatalytic degradation of 4-chlorophenol. J. Molecular Catalysis A: Chemical, 273, 177-185.

Venkatachalam, N., Palanichamy, M., Arabindoo, B., Murugesan, V. (2007). Alkaline earth metal doped nanoporous TiO_2 for enhanced photocatalytic mineralisation of bisphenol. A. J. Catalysis Communications, 8, 1088-1093.

Wang, K., Hisieh, Y., Wu, C., Chang, C. (2000). The pH and anion effects on the heterogeneous photocatalytic degradation of o-methylbenzoic acid in TiO_2 aqueous suspension. Chemosphere, 40, 389-394.

Wang, R., Hashimoto, K., Fujishama, A., Chikuni, M., Kojima, E., Kitamura, A., Shimohigoshi M., Watanabe, T. (1997). Light-induced amphiphilic surfaces. Nature, 388, 431-433.

Wang, W., Zhang, J., Chen, F., He D., Anpo, M. (2008). Preparation and photocatalytic properties of Fe^{2+}-doped Ag@TiO_2 core-shell nanoparticles. J. Colloid Interface Sci., 323, 182-186.

Wang, Z., Chen, C., Wu, F., Zou, B., Zhao, M., Wang, J., Feng, C. (2009). Photodegradation of rhodamine B under visible light by bimetal codoped TiO_2 nanocatalysts. J. Hazard. Mater., 164(2-3), 615-20.

Xu, S., Ng, J., Zhang, X., Bai, H., Sun, D.D. (2010). Fabrication and comparison of highly efficient Cu incorporated TiO_2 photocatalyst for hydrogen generation from water. International journal of hydrogen energy, xxx., 1-8.

Yang, X., Cao, C., Erickson, L., Hohn, K., Maghirang, R., Klabunde, K. (2009). Photocatalytic degradation of Rhodamine B on C-, S-, N-, and Fe-doped TiO_2 under visible-light irradiation. Applied Catalysis B: Environmental., 91, 657-662.

Yoong, L.S., Chong F.K., Dutta, B.K. (2009). Development of copper-doped TiO_2 photocatalyst for hydrogen production under visible light. J. Energy., 34, 1652-1661.

Yu, H., Li, X.J., Zheng S.J., Xua, W. (2006). Photocatalytic activity of TiO_2 thin film non-uniformly doped by Ni, Materials Chemistry and Physics., 97, 59-63.

Zhang, L.C., Cai K.F., Yao, X. (2008). Preparation, characterization and photocatalytic performance of Co/Ni co-doped TiO_2 nanopowders, J. Electroceram., 21, 512-515.